Kinetics of extracellular ATP hydrolysis by microvascular endothelial cells from rat heart

Parviz MEGHJI,*‡ Jeremy D. PEARSON* and Linda L. SLAKEY†

*Vascular Biology Research Centre, Biomedical Sciences Division, King's College London, Campden Hill Road, London W8 7AH, U.K., and †Department of Biochemistry and Molecular Biology, University of Massachusetts, Amherst, MA 01003, U.S.A.

We have characterized the ectonucleotidases that catalyse the reaction sequence ATP → ADP → AMP → adenosine on microvascular endothelial cells cultured from the rat heart. Computer simulation and data fitting of progress of reaction curves showed that depletion of substrate at the cell surface dominates the regulation of the rate of hydrolysis of ATP when it is presented to the cells. Preferential delivery of AMP by ADPase to 5′-nucleotidase makes a significant contribution to the regulation of adenosine production from ATP or ADP. By contrast, we found no evidence for the preferential delivery of ADP from ATPase to ADPase. Feed-forward inhibition of AMP hydrolysis by ADP and/or ATP also modulated the rate of adenosine production. The properties of the ectonucleotidases on rat heart microvascular cells are such that adenosine is produced at a steady rate over a wide range of ATP concentrations.

INTRODUCTION

Adenine nucleotides can be released into the coronary microvasculature from hypoxic or ischaemic myocytes, endothelial cells, damaged blood vessels or aggregating platelets [1]. In the cardiovascular system, extracellular ATP, ADP and adenosine have potent, but often differential, effects. The vasodilator action of ATP and ADP is usually mediated by P_{2Y} receptors on endothelial cells coupled to the production of nitric oxide, whereas adenosine, which also produces vasodilatation, does so by acting directly on adenosine A_2 receptors on smooth-muscle cells. However, on endothelium-denuded vessels, ATP and ADP produce vasoconstriction by acting on P_{2X} receptors on smooth-muscle cells [1]. AMP is essentially inactive [2,3].

Rapid catabolism of ATP occurs on passage through the coronary bed [4–6], and this catabolism is believed to be due to endothelial ectonucleotidases. ATPase, ADPase and 5′-nucleotidase, ectoenzymic activities capable of hydrolysing ATP sequentially to adenosine, are present on many cell types, including cultured endothelial cells from large vessels [7], and these serve to terminate the actions of extracellular ATP and ADP. The adenosine formed is then inactivated by cellular uptake. The opposing effects of adenosine acting on P_1-purinoceptors and ATP acting on P_2-purinoceptors on the same cell types indicates that adenosine modulates the actions of ATP. Hence the rate of hydrolysis of nucleotides by ectonucleotidases is biologically important.

ADP is a potent inhibitor of 5′-nucleotidase. We have previously found in porcine aortic endothelial and smooth-muscle cells, and also in adult rat ventricular myocytes [8–10] that, when kinetic parameters were derived from progress of reaction curves [11,12], best fits were obtained when feed-forward inhibition of 5′-nucleotidase by ADP was taken into account. We have also found that preferential delivery of AMP from ADPase to 5′-nucleotidase makes the rate of adenosine production more efficient when ADP or ATP is the initial substrate than would be predicted from the bulk-phase concentrations [9,10]. Thus the rate of adenosine formation appears to be dependent on the balance between feed-forward inhibition and preferential delivery, and this balance is different in the different cell types we have investigated. Ectoenzymes on microvascular endothelial cells are most likely to metabolize any ATP that is released into the coronary microvasculature. Since the extent of phosphorylation of adenine nucleotides can profoundly modify the physiological effects of extracellular nucleotides, in the present study we have extended the characterization of ectonucleotidases to microvascular endothelial cells from the rat heart.

EXPERIMENTAL

Materials

Collagenase was obtained from Lorne Laboratories U.K., Reading, U.K. (Worthington collagenase, type CLS2) or from Serva (Feinbiochemica G.m.b.H., Heidelberg, Germany). Rabbit anti-(rat liver 5′-nucleotidase) serum was a gift from Dr. J. P. Luzio (Department of Clinical Biochemistry, University of Cambridge, Cambridge, U.K.). AnalaR water used for cell-isolation procedures was obtained from BDH (Poole, Dorset, U.K.). All other materials were obtained from Sigma (St. Louis, MO, U.S.A.) or sources described previously [8] unless indicated otherwise.

Isolation and culture of cells

Coronary endothelial cells were isolated from female Sprague–Dawley rats (200–300 g) using published methods [13] with minor modifications as described below. Briefly, two hearts were perfused with collagenase, and the ventricles were minced, then incubated in the perfusate, which contained collagenase. The cell suspension was filtered and centrifuged briefly to sediment the ventricular myocytes. The supernatant was incubated with trypsin for a further 30 min at 37 °C, then centrifuged. This cell suspension was then centrifuged for 10 min at 250 *g* and the cell

Abbreviations used: HUVEC, human umbilical-vein endothelial cells; PASMC, porcine aortic smooth-muscle cells; FITC, fluorescein isothiocyanate; p[CH_2]pA, adenosine 5′-[$\alpha\beta$-methylene]diphosphate.

‡Present address and address for correspondence: Department of Physiology, Charing Cross and Westminster Medical School, University of London, Fulham Palace Road, London W6 8RF, U.K.

pellet was resuspended in M-199 medium containing 10% foetal-calf serum and 10% newborn-calf serum, and plated in four 1%-gelatin-coated T25 flasks. After 3–4 days the flasks containing confluent monolayers of cells were treated with trypsin and plated into eight uncoated six-well plates, which were then confluent again after a further 4 days.

Characterization of cells

Acetylated low-density-lipoprotein uptake

Cells were washed and incubated for 4 h at 37 °C with acetylated low-density lipoprotein labelled with a fluorescent dye (DiI-Ac-LDL; 10 μg/ml; Biogenesis, Bournemouth, U.K.). Human umbilical-vein endothelial cells (HUVEC; prepared as described previously [14]) were used as positive controls and porcine aortic smooth-muscle cells (PASMC, prepared as described previously by Needham et al. [15]) were used as negative controls.

Von Willebrand factor expression

Cells were washed three times with PBS, fixed and permeabilized in methanol/acetic acid (9:1, v/v) for 2 min at room temperature. Cells were then washed three times with PBS before being incubated with rabbit anti-(human von Willebrand factor) (Sigma; 1:320) for 1 h at room temperature. After a further three washes the cells were incubated with the second antibody, fluorescein isothiocyanate (FITC)-labelled swine anti-rabbit IgG (Dakopatts, Denmark; 1:50) for 30 min at room temperature. HUVEC were used as positive controls.

Lectin cytochemistry

Binding of biotinylated *Bandeiraea* (*Griffonia*) *simplicifolia* Lectin 1 (BS-1 lectin; Isolectin B4; Vector laboratories, Burlingame, CA, U.S.A.) to paraffin sections of rat ventricle was detected as described previously [16]. Monolayers of cultured cells were stained in the same way after being fixed with ice-cold methanol for 45 s.

Smooth-muscle α-actin immunocytochemistry

Cells were washed with PBS and then fixed with ice-cold methanol for 45 s. They were then washed three times with PBS again before being incubated with monoclonal anti-(smooth-muscle α-actin) mouse ascites fluid (Sigma; 1:50) for 60 min. After a further three washes, the cells were incubated with the second antibody, namely FITC-conjugated rabbit anti-mouse IgG (Dakopatts; 1:50) for 30 min. PASMC were used as positive controls and HUVEC as negative controls.

Cytokeratin immunocytochemistry

The possibility that the endothelial-cell preparation was contaminated by mesothelial cells was investigated by immunofluorescence staining using mouse monoclonal antibodies directed against human cytokeratins 10, 17 and 18 (Dakopatts; clone MNF116) or 4, 5, 6, 8, 10, 13 and 18 (Sigma, clone C-11). Cells from 4- and 9-day-old cultures were fixed with either ice-cold methanol for 2 min or with methanol/acetic acid (9:1, v/v) for 2 min at room temperature. They were washed three times with PBS and incubated with antibodies (Dakopatts; 1:100–1:10 or Sigma; 1:100) for 60 min. The cells were then washed three times and incubated with the second antibody, FITC-conjugated rabbit anti-mouse IgG (Dakopatts; 1:50) for 30 min. HUVEC were used as negative controls. Frozen sections of rat lung were used as positive controls.

Prostacyclin production

Confluent cell monolayers in six-well plates were rinsed with Hepes-buffered Dulbecco's Modified Eagle's Medium and incubated in 1.2 ml of the same buffer. For estimates of basal values of prostaglandin release, 0.2 ml samples were removed at 5 min and 30 min. Agonists (0.2 ml) were then added and the medium removed 5 min later to estimate stimulated release. Prostacyclin was detected as its stable hydrolysis product, 6-oxoprostaglandin $F_{1\alpha}$, by radioimmunoassay [17].

Cell viability

Cellular integrity was estimated in initial experiments by measuring the release of lactate dehydrogenase activity in the supernatant medium and comparing it with the total enzyme activity in cells lysed with 10 mM Tes/NaOH, pH 7, containing 0.1% Triton X-100 [18]. At least 95% of the cells remained intact after incubation at 37 °C for 60 min on an orbital shaker.

Incubations

Cells were preincubated for 30 min with 10 μM dipyridamole unless otherwise stated. They were then rinsed three times with Krebs/Hepes buffer composed of 125 mM NaCl, 2.6 mM KCl, 1.2 mM KH_2PO_4, 1.2 mM $MgSO_4$, 10 mM Hepes, 1 mM $CaCl_2$ and 0.2% BSA, pH 7.4, equilibrated with air, and placed in 0.9 ml of the same buffer at 37 °C on an orbital shaker (1.5 orbits/s). Incubations were started by adding buffer (100 μl) containing unlabelled nucleotide, and 0.22 MBq [^{3}H]AMP (sp. radioactivity 0.56 TBq/mmol) or [2,8-^{3}H]ADP (sp. radioactivity 1.2 TBq/mmol) or [2,8,-^{3}H]ATP (sp. radioactivity 1.5 TBq/mmol) and dipyridamole. The distribution of radiolabel in each tracer used as the substrate (e.g. the amount of label associated with ATP, ADP and AMP in the nominal ATP tracer) was determined and an unlabelled nucleotide mixture was prepared to match [10]. Subsamples (40 μl) of the incubation mixture were removed at timed intervals and, for TLC, added to 10 μl of unlabelled carrier (5 mM each of ATP, ADP, AMP, IMP, adenosine, inosine and hypoxanthine). Incorporation of adenosine into cellular nucleotides was measured as described previously [19].

Nucleotide and nucleoside analysis

In most experiments, catabolism of [^{3}H]nucleotides was measured by TLC of the subsamples. Aliquots (20 μl) of the subsamples were spotted on to silica-gel-coated glass plates, and nucleotides were separated as described previously [20]. Radioactivity in each lane was monitored directly with a Berthold LB2842 linear analyser [6]. In some experiments, only unlabelled substrate was used and nucleotide analysis was performed by HPLC as previously described [8].

Kinetic analysis

The algorithms and programs used are described in detail elsewhere [11,12]. It was assumed that each reaction for the pathway ATP → ADP → AMP → adenosine is catalysed by one kinetically distinct ectonucleotidase and that all reactions occur in the same kinetic compartment, having access to all the substrates and products. Initial concentrations of all substrates and test values for the kinetic parameters are specified, and the time course of the reaction is simulated by numerical integrations over a succession of short intervals. Predicted time courses were compared with data sets, and kinetic parameters were altered until a good fit was obtained between simulated and observed

time courses, thus providing estimates of apparent kinetic constants.

RESULTS

Cell characterization

Piper et al. [13] have previously characterized endothelial cells prepared from rat heart by the methods used here, by their characteristic 'cobblestone' morphology, weakly positive expression of von Willebrand factor, ability to take up acetylated low-density lipoprotein, and lack of expression of smooth-muscle α-actin. We confirmed these findings, and additionally observed positive binding of BS-1 lectin in endothelial cells of rat ventricular tissue and in the cultured cells, and no detectable expression of cytokeratins (results not shown). We also detected prostacyclin synthesis: basal release of 55 ± 46 pg/min/10^6 cells (mean $\pm$ S.E.M., $n = 5$) was increased by the calcium ionophore A23187 (1 μM) to 550 ± 190 pg/min per 10^6 cells ($n = 5$), by bradykinin (100 nM) to 390 ± 130 pg/min per 10^6 cells ($n = 4$) or by ATP (50 μM) to 560 pg/min per 10^6 cells (mean result for two experiments).

Incorporation of adenosine into cellular nucleotides

Rat coronary endothelial cells, when incubated with 10 μM [^{3}H]adenosine for 1 h, incorporated 71.2 ± 4.3 pmol of adenosine/10^6 cells (mean $\pm$ S.E.M.; $n = 3$) . Dipyridamole (10 μM) inhibited this incorporation by 51 ± 10% (mean $\pm$ S.E.M.; $n = 3$) and was included in the remainder of the experiments to minimize adenosine uptake and intracellular metabolism.

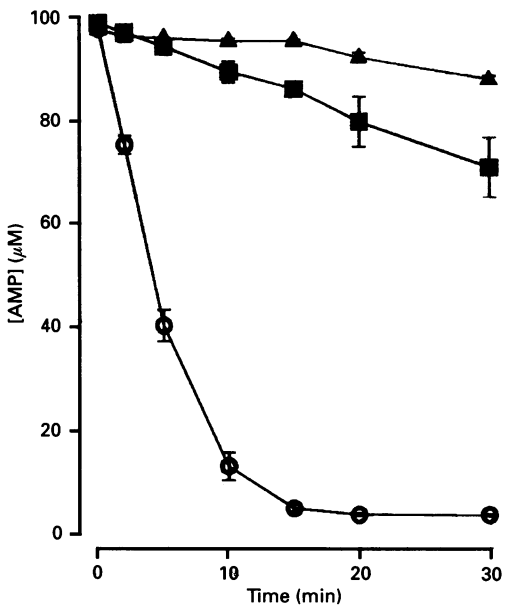

Figure 2 Inhibition of AMP hydrolysis

Cells were preincubated with 10 μM dipyridamole alone (○) or together with either 10 μM p[CH_2]pA (■) or with antiserum (1:100 dilution in M-199 medium containing 10% foetal-calf serum and 10% newborn-calf serum) (▲) for at least 30 min and then washed with Krebs/Hepes buffer before being incubated with [^{3}H]AMP (100 μM) and dipyridamole (10 μM) alone or together with p[CH_2]pA. Values are means $\pm$ S.D. for triplicate observations. The data are representative of those obtained from three different experiments. AMP hydrolysis was significantly ($P < 0.05$) inhibited by the antiserum or p[CH_2]pA at all time points tested (Student's t test for paired samples).

Pattern of nucleotide hydrolysis

A representative time course of hydrolysis of 300 μM ATP by coronary endothelial cells is illustrated in Figure 1(a). The decrease in ATP concentration with time was accompanied by a rise in ADP concentration. Little AMP accumulated, and there was rapid production of adenosine. When ADP was the initial substrate, again there was little AMP accumulation and adeno-

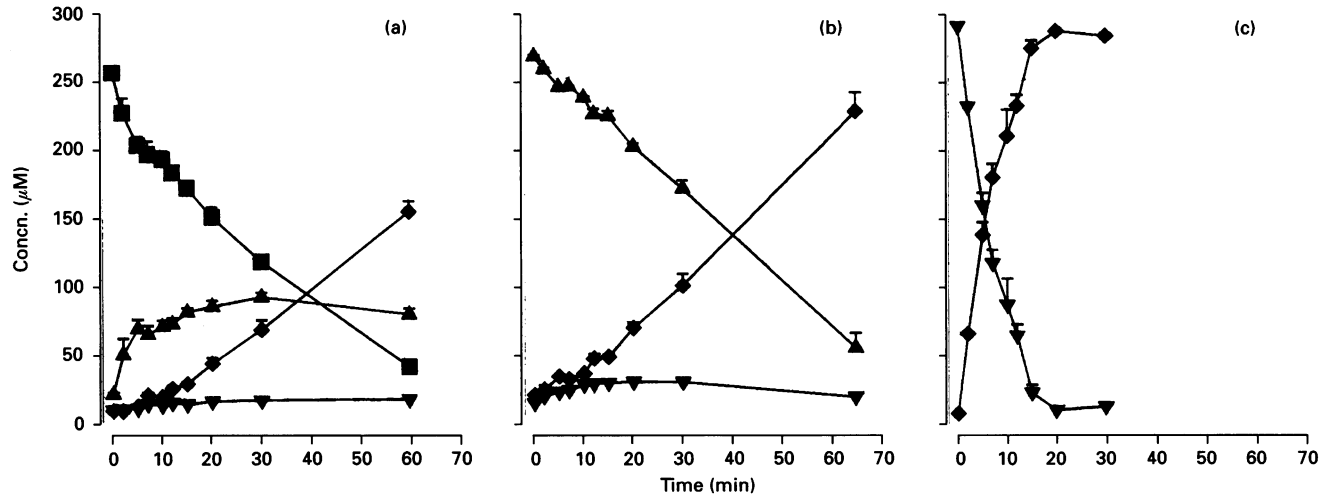

Figure 1 Time course of product formation from catabolism of exogenous nucleotides by rat heart microvascular endothelial cells

Cells were incubated with (**a**) [^{3}H]ATP (260 μM), (**b**) [^{3}H]ADP (270 μM) and (**c**) [^{3}H]AMP (290 μM) in the presence of 10 μM dipyridamole, and subsamples were removed at timed intervals and assayed by TLC as described in the text. ■, ATP; ▲, ADP; ▼, AMP; ◆, AMP metabolites. Values are means $\pm$ S.D. for triplicate observations. In this experiment the apparent K_m values derived from progress of reaction curves for each nucleotide used as initial substrate were as follows: ATPase $\geqslant$ 10 mM; ADPase, 70 μM; AMPase, 1300 μM. The data are representative of those obtained from at least three different experiments. K_m values were also determined using other substrate concentrations (the data are summarized in Table 1).

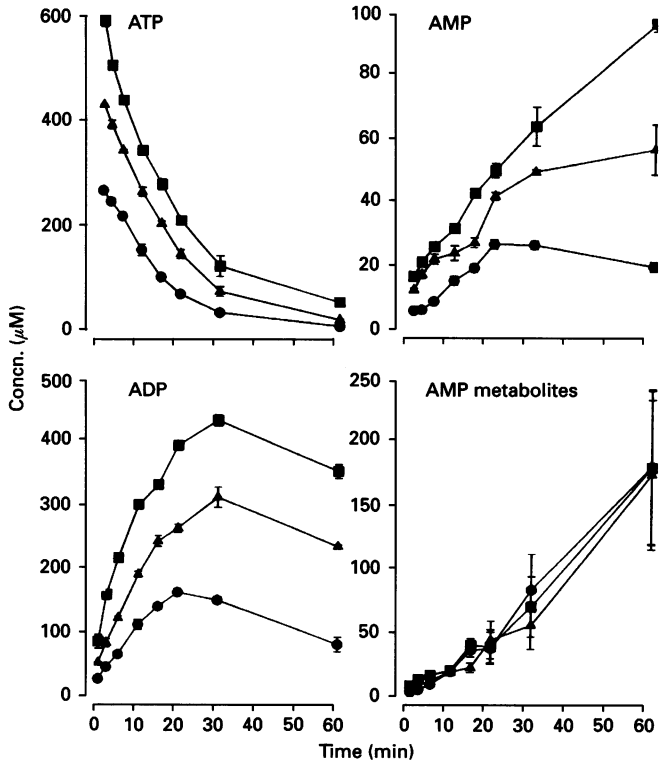

Figure 3 Relationship between hydrolysis pattern and initial ATP concentration

Cells were preincubated with 10 μM dipyridamole. The time course of hydrolysis was measured for three initial ATP concentrations [270 μM (●); 430 μM (▲) and 590 μM (■)] in the presence of dipyridamole (10 μM). Values are means ± S.D. for triplicate observations. The data are representative of those from three different experiments.

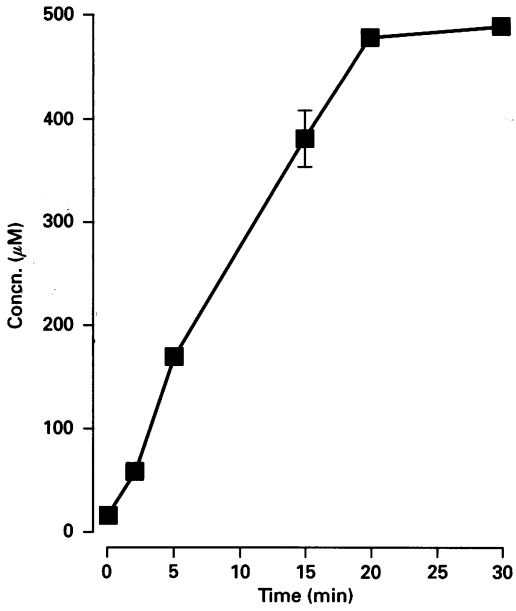

Figure 4 Production of adenosine by hydrolysis of AMP

Cells were preincubated with 10 μM dipyridamole. The time course of adenosine production was measured in the presence of dipyridamole when 500 μM AMP (■) was the initial substrate. Values are means ± S.D. for triplicate observations. The apparent K_m value for 5′-nucleotidase in this experiment was 20 μM. K_m values were also determined using other substrate concentrations (the data are summarized in Table 1).

sine was rapidly produced (Figure 1b). When AMP was the initial substrate, the rapid disappearance of AMP was mirrored by the production of adenosine (Figure 1c). IMP was not detected. Inosine accounted for less than 15% of total AMP metabolites, regardless of whether the initial substrate was ATP, ADP or AMP. Hypoxanthine was not detected in any experiment. Adenosine and inosine data have been summed and are presented as AMP metabolites. The sequential accumulation of ADP, AMP and adenosine from ATP, and the hydrolysis pattern of each nucleotide when it was presented as initial substrate, suggest the presence of three enzymic activities: ATPase, ADPase and 5′-nucleotidase. β-Glycerophosphate (0.5–1 mM) or *p*-nitrophenyl phosphate (1 mM) did not inhibit catabolism of ATP (10 μM), ADP (10 μM) or AMP (10 μM), demonstrating that non-specific phosphatases are not responsible for the hydrolysis of these nucleotides.

Inhibition of nucleotide hydrolysis

The ability of ADP or a non-degradable analogue of ADP, adenosine 5′-[αβ-methylene]diphosphate (p[CH_2]pA), to inhibit 5′-nucleotidase has been used to distinguish this enzyme from other phosphatases in a wide variety of tissues [21]. Hydrolysis of 100 μM AMP by coronary endothelial cells was inhibited by p[CH_2]pA or rabbit anti-(rat liver 5′- nucleotidase) serum (Figure 2). When ATP or ADP was the initial substrate, the antiserum did not affect the rate of hydrolysis of ATP or ADP, but caused a decrease in adenosine production and an increase in accumulation of AMP (results not shown).

Feed-forward inhibition of 5′-nucleotidase by ATP and ADP

As the initial concentration of ATP presented to the microvascular endothelial cells was increased (270–590 μM), the rate of appearance of the subsequent metabolite ADP also increased (Figure 3). ADP was metabolized slowly, accounting for nearly 60% of the products formed 30 min after 270 μM ATP was added ($n = 3$). The rate of appearance of AMP also increased, but the rate of conversion of AMP into adenosine remained constant as the ATP concentration was increased from 270 μM to 590 μM (Figure 3). By contrast, when AMP was the initial substrate, adenosine was produced rapidly and the reaction was complete within 20 min even with initial AMP concentrations as high as 500 μM (Figure 4).

Data analysis by modelling progress of reaction curves

The kinetic parameters were estimated from progress of reaction curves. In seven out of the eight experiments, even at high initial substrate concentrations, the reaction followed pseudo-first-order kinetics, suggesting that hydrolysis is rate-limited by the supply of substrate from the bulk phase. The apparent values of K_m for the ATPase were thus too high to be estimated accurately (Table 1), similarly to our findings with adult rat ventricular myocytes [10]. This effect was less apparent in the hydrolysis of ADP or AMP. Concentrations of substrates produced in the microenvironment of an enzyme can be significantly greater than the observed concentrations in the bulk phase. In this case the

Table 1 Comparison of apparent kinetic parameters* found using ATP, ADP or AMP as initial substrates

Values are means ± S.E.M. for the numbers indicated. $V_{max.}$ cannot be determined under these conditions. *$P < 0.01$; significantly different from when AMP was the initial substrate using the Mann–Whitney U-test. Kinetic parameters obtained for ADP were the same whether ADP was the initial substrate or was supplied from ATP.

Initial [substrate]	$K_{m(ATPase)}$ (μM)	$V_{max.}/K_{m(ATPase)}$ (ml/min per 10^6 cells)	$K_{m(ADPase)}$ (μM)	$V_{max.(ADPase)}$ (nmol/min per 10^6 cells)	$V_{max.}/K_{m(ADPase)}$ (ml/min per 10^6 cells)	$K_{m(AMPase)}$ (μM)	$V_{max.(AMPase)}$ (nmol/min per 10^6 cells)	$V_{max.}/K_{m(AMPase)}$ (ml/min per 10^6 cells)	K_i† (μM)
AMP ($n = 11$) 100–500 μM						245 ± 120	74 ± 18	0.4 ± 0.04	
ADP ($n = 5$) 100–500 μM			510 ± 300	8.1 ± 2.2	0.06 ± 0.04	11.0 ± 0.5*	193 ± 23*	18 ± 3*	1.5 ± 0.3
ATP (n = 8) 100–700 μM	≫ 10000‡	0.09 ± 0.01‡	390 ± 150	13 ± 2.9	0.1 ± 0.06	10.3 ± 1.7*	210 ± 50*	22 ± 5*	1.3 ± 0.2

*Values for kinetic parameters varied substantially between experiments.
†K_i is the inhibition constant for competitive inhibition of 5′-nucleotidase by ADP.
‡Fitting of data was arbitrarily stopped when the K_m values for ATPase exceeded 10 mM.

apparent K_m values found for ADPase and 5′-nucleotidase when ADP or AMP are supplied as initial substrates will be different from those found when they are preferentially supplied from the preceding reactions. Estimates of K_m values of ADPase made by fitting observed levels of ADP when it was supplied by ATPase yielded apparent K_m values that were very similar to those obtained when ADP itself was the initial substrate (Table 1). Kinetic parameters for 5′-nucleotidase were estimated by fitting data to a model where competitive inhibition of the enzyme by ADP was taken into account. When the initial substrate was ATP or ADP, the apparent K_m for AMP was at least 10-fold lower than when AMP was the initial substrate (Table 1). The apparent K_i values for ADP that gave the best fit to the data were the same whether ATP or ADP was the initial substrate. These results are consistent with a model in which the concentration of ADP at the cell surface is the same when ATP is supplied initially or when ADP is the initial substrate. Thus there is evidence for preferential delivery of substrate to 5′-nucleotidase, but not to ADPase.

DISCUSSION

The rat heart microvascular cells that we have prepared using the method of Piper et al. [13] appear to be similar to those cells prepared by other workers using different methods of cell isolation [22,23], and we have provided further characterization of the cells (positive BS-1 lectin binding, prostacyclin synthesis and lack of expression of cytokeratins). The last property distinguishes these cells from mesothelial cells [24,25].

ATP pyrophosphohydrolase activity has been detected in perfusion studies of guinea-pig [26] and rat hearts [6]. Low activity was observed on pig aortic endothelial cells [27], and the enzyme was not detectable on pig aortic smooth-muscle cells [28] or rat ventricular myocytes [10]. We have shown here that rat heart coronary endothelial cells have ectonucleotidase activities capable of hydrolysing ATP, ADP and AMP. Hydrolysis of AMP was inhibited by specific 5′-nucleotidase antiserum or the non-hydrolysable ADP analogue p[CH_2]pA. When ATP or ADP was the initial substrate, very little AMP accumulated. However, when 5′-nucleotidase was inhibited, AMP accumulated and adenosine formation was inhibited, demonstrating that nucleotide catabolism to adenosine involves 5′-nucleotidase. In the present study, direct conversion of ATP into AMP did not occur to any significant extent. When ATP was catabolized by the cells, ADP was formed immediately, whereas AMP was only formed after a time lag (Figure 1a). Thus the pattern of hydrolysis of ATP, ADP and AMP indicates the presence of three enzymic activities: ecto-ATPase, ecto-ADPase and ecto-5′-nucleotidase.

Since the extent of phosphorylation can profoundly modify the physiological effects of extracellular adenine nucleotides, we hypothesized that the time course of their hydrolysis would be regulated and that the pattern of their hydrolysis might differ in different cell types. We have now examined in detail the time course of the extracellular hydrolysis sequence ATP → ADP → AMP → adenosine in four different cell types, namely rat microvascular endothelial cells (the present study), porcine aortic endothelial and smooth-muscle cells [8,9] and adult rat ventricular myocytes [10]. One of the main conclusions from our studies is that these cell types differ markedly in the rate at which they produce adenosine from ATP or ADP. This rate is determined by the balance between feed-forward inhibition of 5′-nucleotidase by ADP (and/or ATP) and preferential delivery of AMP from ADPase to 5′-nucleotidase. It remains to be determined whether some of the differences that we have observed can be attributed to species differences or whether they are cell-specific.

In all four cell types we find kinetic evidence that feed-forward inhibition of 5′-nucleotidase decreases the efficiency of adenosine production from ATP and ADP. In contrast, the counterbalancing effect of preferential delivery of locally produced AMP, likely to occur when the enzymes are located in close proximity, is different in each cell type. This is reflected in the extent to which the production of adenosine is more efficient when ADP or ATP is the initial substrate than is predicted from the observed bulk-phase AMP concentrations, and is pictorially represented in Scheme 1. Porcine aortic smooth-muscle and endothelial cells [8,9], which have similar capacities to hydrolyse ATP but differ greatly in their rates of production of adenosine from ATP, provide extreme examples of the relative importance of feed-forward inhibition and preferential delivery. In porcine aortic endothelial cells, the effect of feed-forward inhibition was predominant. Adenosine was only produced after a long lag when the concentrations of ATP and ADP had decreased substantially, and there was no evidence for preferential delivery of either ADP or AMP ([8]; Scheme 1a). In smooth-muscle cells, preferential delivery of substrates outweighed the effect of feed-forward inhibition of 5′-nucleotidase by ADP, and adenosine was produced immediately and rapidly at all initial concentrations of ATP or ADP ([9]; Scheme 1c).

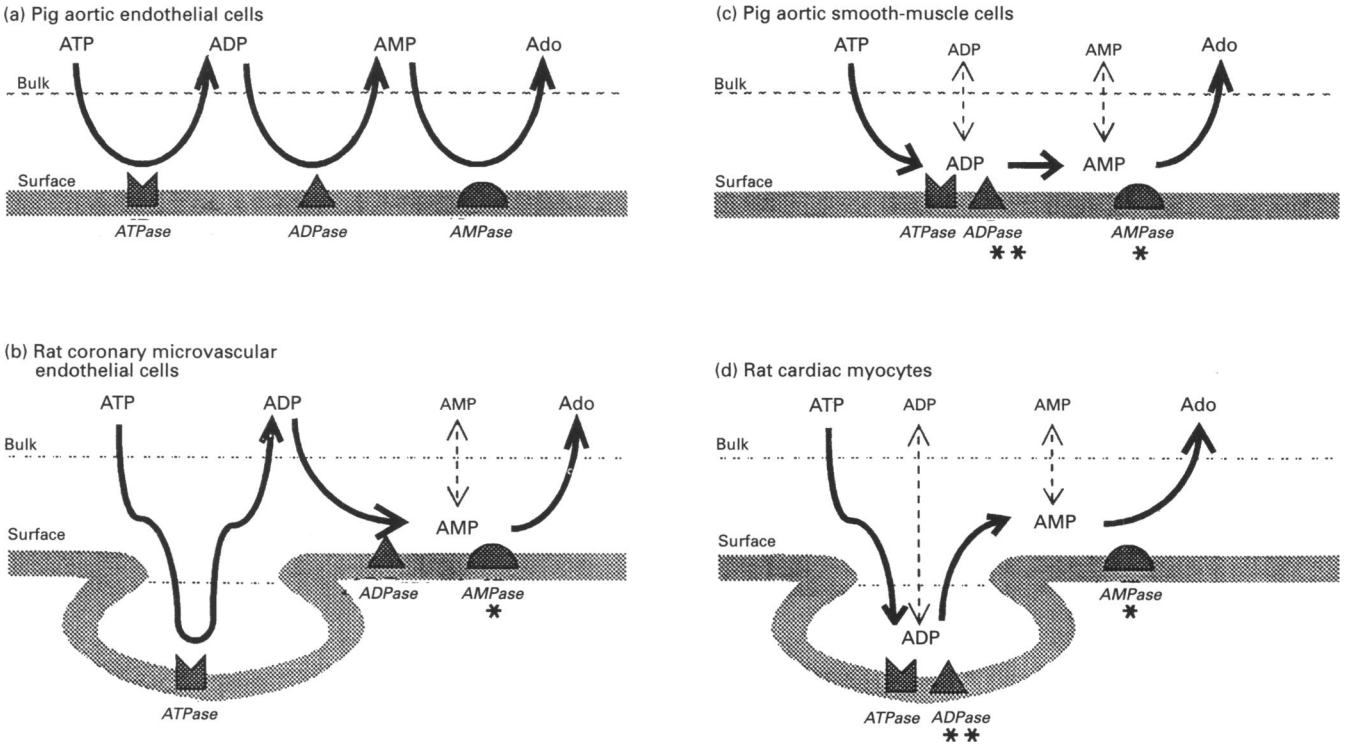

Scheme 1 Representation of the possible spatial relationships between ectonucleotidases on different cardiovascular cell types, deduced from kinetic analysis of progress of reaction data ([8–10]; the present study)

The catabolic pathway is highlighted to indicate (i) where preferential delivery of surface-phase substrate occurs (*evidence of preferential delivery; **evidence of highly preferential delivery) and (ii) the apparently poor accessibility of ATPase (**b**,**d**) and ADPase (**d**) to bulk-phase substrates. The rate of adenosine (Ado) production is also influenced in all cell types by feed-forward inhibition of 5′-nucleotidase (AMPase) by ADP (see the text for details).

Both preferential delivery of substrate and feed-forward inhibition of 5′-nucleotidase had a significant impact on adenosine production by cardiac myocytes ([10]; Scheme 1d). Preferential delivery of substrate from the preceding reaction had less impact on delivery of AMP from ADPase to 5′-nucleotidase than it did on the delivery of ADP from ATPase to ADPase in porcine aortic smooth-muscle cells and rat cardiac myocytes ([9,10]; Scheme 1). In the present study with rat coronary endothelial cells, there was no evidence for the preferential delivery of ADP from ATPase to ADPase, but AMP was preferentially delivered from ADPase to 5′-nucleotidase (Table 1; Scheme 1b). Feed-forward inhibition was also important. Interestingly the properties of the enzymes on rat heart microvascular cells, unlike those of the other three cell types, are such that adenosine is produced at a relatively constant rate from a range of initial ATP concentrations (Figure 3).

The ATPase reaction in rat coronary endothelial cells followed pseudo-first-order kinetics, and the estimated K_m values are thus very high, suggesting that the pool of substrate available to the enzyme is not in equilibrium with the bulk phase. We have previously made similar observations for both the ATPase and ADPase in ventricular myocytes [10]. With rat ventricular myocytes, we additionally demonstrated a lack of proportionality of rate of hydrolysis of ATP to cell number, further suggesting a depletion of substrate from the microenvironment of the enzyme [10]. Possibly these enzymes are located in caveloae or pits on the cell surface, where local depletion of substrate is likely to occur (Schemes 1b and 1d). Pitted surfaces have been described for other cell types and may serve to concentrate low-molecular-mass substances at the cell surface [29]. When ATP is released from endothelial cells rather than supplied exogenously, the outcome may be different, as the pits will result in a concentration of ATP at the cell surface. Alternatively, clusters of molecules of a single enzyme on the cell surface would also result in rapid depletion of the substrate from the immediate vicinity of the enzyme, and thus give rise to first-order kinetics. Ecto-ATPase purified from rat liver has a much lower apparent K_m (100–200 μM; [30]). The lowest apparent K_m value we observed for AMPase (20 μM; Table 1) is approximately that of the purified enzyme [31]. The rest of the values tended to be higher. The apparent K_m values for ADPase and AMPase varied substantially between individual experiments. Higher apparent K_m values were associated with higher apparent $V_{max.}$ values (results not shown). This suggests that local depletion of substrate occurs even for ADPase and AMPase and that this varies in extent from preparation to preparation. The extent of local substrate depletion was very different for the ATPase and the ADPase, although their efficiencies were similar (Table 1); indeed, as indicated in Scheme 1(b) and Table 1, the kinetic data suggest that ADP generated from ATPase by the microvascular endothelial cells (as in aortic endothelial cells; Scheme 1a) is not distinguishable by the ADPase from ADP in the bulk phase.

The relative amounts of ATPase and ADPase activities varied somewhat from one cell preparation to another, as is evident, for example, in the different extents of ADP accumulation observed at 270 μM ATP in Figures 1 and 3. These data suggest that the

ATPase and ADPase are separate enzymes. Adenosine 5′-[$\beta\gamma$-imido]triphosphate more potently inhibits the rate of hydrolysis of ADP than of ATP in rat ventricular myocytes [10], porcine aortic endothelial cells [8] and human leucocytes [32], as would be the case if the two enzymic activities are due to separate enzymes. However, the purified (Ca^{2+}-Mg^{2+})-ecto-ATPase from rat liver [33] and the ATPase from bovine aorta [34] have broad nucleotide specificity and are able to hydrolyse both ATP and ADP to a similar extent. Hydrolysis of ATP and ADP by the same enzyme would explain the very efficient hydrolysis of ADP produced from ATP in rat ventricular myocytes [10] and porcine aortic smooth-muscle cells ([9]; Schemes 1c and 1d). However, the kinetic evidence summarized above, and the lack of preferential delivery of ADP by ATPase to ADPase in the present study and also in porcine aortic endothelial cells [8] support the hypothesis that the ATPase and ADPase activities are due to separate enzymes on endothelial cells.

In conclusion, we have examined the kinetic pattern of hydrolysis of extracellular nucleotides by ectonucleotidases on rat coronary microvascular cells, and have deduced that there are substantial differences in the organization of ectonucleotidases on these cells by comparison with other cardiovascular cells. In addition to significant contribution of surface effects to the measured kinetic constants, these cells uniquely operate to generate adenosine at a relatively constant rate when presented with a wide range of concentrations of ATP (or ADP) as the initial substrate. This may be important for the regulation of the effects of adenosine on the heart, implicated in responses to hypoxia or ischaemia [1].

This work was supported by National Institutes of Health Grant HL-31854 and the British Heart Foundation. We thank Dr. H. M. Piper for advice in establishing rat coronary endothelial cell cultures, to Sue Barker for help in preparation and staining of frozen sections, to Kirtida Patel for technical assistance and to Tom Pearson for graphics.

REFERENCES

1 Olsson, R. A. and Pearson, J. D. (1990) Physiol. Rev. **70**, 761–845
2 Bruns, R. F. (1990) Ann. N. Y. Acad. Sci. **603**, 211–226
3 Ragazzi, E., Wu, S.-N., Shryock, J. and Belardinelli, L. (1991) Circ. Res. **68**, 1035–1044
4 Paddle, B. M. and Burnstock, G. (1974) Blood Vessels **11**, 110–119
5 Ronca-Testoni, S., and Borghini, F. (1982) J. Mol. Cell. Cardiol. **14**, 177–180
6 Fleetwood, G., Coade, S. B., Gordon, J. L. and Pearson, J. D. (1989) Am. J. Physiol. **256**, H1565–H1572
7 Pearson, J. D., Carleton, J. S. and Gordon, J. L. (1980) Biochem. J. **190**, 421–429
8 Gordon, E. L., Pearson, J. D. and Slakey, L. L. (1986) J. Biol. Chem. **261**, 15496–15504
9 Gordon, E. L., Pearson, J. D., Dickinson, E. S., Moreau, D. and Slakey, L. L. (1989) J. Biol. Chem. **264**, 18986–18992
10 Meghji, P., Pearson, J. D. and Slakey, L. L. (1992) Am. J. Physiol. **263**, H40–H47
11 Slakey, L. L., Cosimini, K., Earls, J. P., Thomas, C. and Gordon, E. L. (1986) J. Biol. Chem. **261**, 15505–15507
12 Slakey, L. L., Eikenberry, J., Hayes, D. R. and Gordon, E. L. (1989) J. Biol. Chem. **264**, 18993–18995
13 Piper, H. M., Spahr, R., Mertens, S., Krutzfeldt, A. and Watanabe, H. (1990) in Cell Culture Techniques in Heart and Vessel Research (Piper, H. M., ed.), pp. 158–177, Springer–Verlag, Heidelberg
14 Jaffe, E. A., Nachman, R. L., Becker, C. G. and Minick C. R. (1973) J. Clin. Invest. **52**, 2745–2756
15 Needham, L., Cusack, N. J., Pearson, J. D. and Gordon, J. L. (1987) Eur. J. Pharmacol. **134**, 199–209
16 Alroy, J., Goyal, V. and Skutelsky, E. (1987) Histochemistry **86**, 603–607
17 Ager, A., Gordon, J. L., Moncada, S., Pearson, J. D., Salmon, J. A., and Trevethick, M. A. (1982) J. Cell. Physiol. **110**, 9–17
18 Meghji, P., Holmquist, C. A. and Newby, A. C. (1985) Biochem. J. **229**, 799–805
19 Meghji, P., Skladanowski, A. C., Newby, A. C., Slakey, L. L. and Pearson, J. D. (1993) Biochem. J. **291**, 833–839
20 Norman, G. A., Follett, M. J. and Hector, D. A. (1974) J. Chromatogr. **90**, 105–111
21 Burger, R. M., and Lowenstein, J. M. (1975) Biochemistry **14**, 2362–2366
22 Diglio, C. A., Grammas, P., Giacomelli, F. and Wiener, J. (1988) Tissue Cell **20**, 477–492
23 Nishida, M., Carley W. W., Gerritsen, M. E., Ellingsen, O., Kelly, R. A. and Smith, T. W. (1993) Am. J. Physiol. **264**, H639–H652
24 Van Hinsbergh, V. W. M., Kooistra, T., Scheffer, M. A., Van Bockel, J. H. and Van Muijen, G. N. P. (1990) Blood **75**, 1490–1497
25 Pronk, A., Leguit, P., Hoynck van Papendrecht, A. A. G. M., Hagelen, E., Van Vroonhoven, T. J. M. V. and Verbrugh, H. A. (1993) In Vitro Cell. Dev. Biol. **29A**, 127–134
26 Imai S., Chin, W.-P. Jin, H. and Nakazawa, M. (1989) Pfluegers Arch. **414**, 443–449
27 Cusack, N. J., Pearson, J. D., and Gordon, J. L. (1983) Biochem. J. **214**, 975–981
28 Pearson, J. D., Coade, S. B. and Cusack, N. J. (1985) Biochem. J. **230**, 503–507
29 Anderson, R. G. W. (1993) Current Opin. Cell Biol. **5**, 647–652
30 Lin, S.-H. (1985) J. Biol. Chem. **260**, 10976–10980
31 Naito, Y., and Lowenstein, J. M. (1981) Biochemistry **20**, 5188–5194
32 Coade, S. B., and Pearson, J. D. (1989) Circ. Res. **65**, 531–537
33 Lin, S. -H., and Russell, W. E. (1988) J. Biol. Chem. **263**, 12253–12258
34 Yagi, K., Shinbo, M., Hashizume, M., Shimba, L. S., Kurimura, S. and Miura, Y. (1991) Biochem. Biophys. Res. Commun. **180**, 1200–1206

Received 5 September 1994/1 February 1995; accepted 16 February 1995